Journal of Biomedical Optics 9(1), 154–161 (January/February 2004)

Calculation of ocular single-pass modulation transfer function and retinal image simulation from measurements of the polarized double-pass ocular point spread function

Katsuhiko Kobayashi
Topcon Corporation
Research and Development Center
75-1, Hasunuma-cho, Itabashi-ku
Tokyo, 175-8580
and
Chiba University Research Center for Frontier Medical Engineering
1-33, Yayoi-cho, Inage-ku
Chiba-shi
Japan
E-mail: k.koba@topcon.co.jp

Masahiro Shibutani
Gaku Takeuchi
Topcon Corporation
Research and Development Center
75-1, Hasunuma-cho, Itabashi-ku
Tokyo, 175-8580
Japan

Kazuhiko Ohnuma
Yoichi Miyake
Chiba University Faculty of Engineering
Chiba University Research Center for Frontier Medical Engineering
1-33, Yayoi-cho
Inage-ku
Chiba-shi
Japan

Kazuno Negishi
Keio University School of Medicine
Department of Ophthalmology
35 Shinanomachi, Shinjuku-ku
Tokyo 160-8582
Japan

Kenji Ohno
Toru Noda
National Tokyo Medical Center
Department of Ophthalmology
2-5-1, Higashigaoka, Meguro-ku
Tokyo, 152-0982
Japan

Abstract. The single-pass modulation transfer function (MTF_{sgl}) is an important numerical parameter that can help elucidate the performance and some processes of the human visual system. In previous studies, the MTF_{sgl} was calculated from double-pass point spread function (PSF) measurements. These measurements include a depolarized reflection component from the retina that introduces a measurement artifact, and they require long acquisition times to allow averaging to reduce speckle. To solve these problems, we developed a new ocular PSF analysis system (PSFAS) that uses polarization optics to eliminate the depolarized retinal reflection component, and a rotating prism to increase measurement speed. Validation experiments on one patient showed that the MTF_{sgl} measured by PSFAS agrees closely with the MTF calculated from contrast sensitivity measurements. A simulated retinal image was calculated by convolution of Landolt rings with the calculated single-pass PSF provided by the PSFAS. The contrast characteristic then was calculated from the simulated retinal images. These results indicate that the MTF_{sgl} obtained using the PSFAS may be a reliable measure of visual performance of the optics of the eye, including the optical effects of the retina. The simulated retinal images and contrast characteristics are useful for evaluating visual performance.
[DOI: 10.1117/1.1627777]

Keywords: modulation transfer function; point spread function; polarization; double-pass technique; retinal image; retinal image contrast.

Paper 103010 received Mar. 31, 2003; revised manuscript received Jul. 30, 2003; accepted for publication Jul. 31, 2003.

1 Introduction

A number of researchers have proposed calculating the eye's modulation transfer function (MTF) from measurements of the ocular point spread function (PSF). Santamaria et al.[1] initially established the principles of this technique, which provides the MTF of the eye. Further theoretical and technical developments and extensive studies by Artal et al.,[2] Navarro et al.,[3–5] and Williams et al.[6] helped establish the technique and demonstrate its usefulness as a research tool for evaluating visual performance. The ocular PSF and MTF also can be calculated from ocular wavefront aberration data. Recently, simulated retinal images were calculated by convolving an arbitrary optotype, such as the letter E, with the eye's PSF derived from clinical measurements using a wavefront aberrometer.[7]

These techniques and calculations can help evaluate the performance of the optical system from the cornea to the–retina, but the reliability of creating a model of the perceived retinal image remains unclear. The interpretation of simulated retinal images calculated from wavefront aberrometry remains problematic, particularly because the correspondence of the

1083-3668/2004/$15.00 © 2004 SPIE

calculated MTF with the true visual performance is still not clearly understood. MTF alone characterizes only the optical behavior of the refractive components of the eye, including at most the direction feature of the retinal reflection. Another problem is that the exact position on the retina of the simulated retinal image is not known.

The reflection from the fundus of the human eye includes both a polarized and a depolarized component.[8,9] Hence it is desirable that the depolarized reflection component of the retina, which introduces an artifact in the measured MTF, be fully eliminated. The polarized component originates at the surface of the retinal pigment epithelium (RPE) at a long wavelength near infrared.[6,10,11] The depolarized component is caused by the sclera and choroid. While the polarized component forms a high-contrast retinal image on the external limiting membrane, the depolarized component forms a low-contrast image near the surface of the RPE.

According to Williams et al.[6] and O'Leary and Millodot,[12] human subjects can perceive both the polarized and depolarized image, but the depolarized component has little effect on the MTF. However, to obtain a more reliable value of the single-pass MTF (MTF_{sgl}) of the human eye, only the polarized component of the retinal reflection should be taken into account in the calculation of the MTF_{sgl} from the double-pass PSF (PSF_{dbl}). The double-pass PSF measurement system must therefore selectively measure the PSF_{dbl} of the polarized component of the reflected image. For this purpose, we developed an optical system, called the point spread function analysis system (PSFAS), for measuring the eye's MTF[13–15] that eliminates the depolarized reflection component. Preliminary experiments demonstrated the reliability of the MTF_{sgl} produced by the polarized PSF_{dbl}.[16] In this paper, we present the optical principles and design of the PSFAS and the experiments to evaluate the performance of the system compared with traditional methods.

The following definitions and notations are used in the text for the MTF and the PSF:

$i_{dbl}(x,y)$ is the two-dimensional double-pass PSF (PSF_{dbl}) image captured by the CCD camera

$I_{dbl}(U,V)$ is the two-dimensional double-pass MTF (MTF_{dbl}) calculated by taking the Fourier transform of $i_{dbl}(x,y)$,

$I_{sgl}(U,V)$ is the two-dimensional single-pass MTF (MTF_{sgl}) equal to the square root of $I_{dbl}(U,V)$, and

$i_{sgl}(x,y)$ is the two-dimensional single-pass PSF (PSF_{sgl}) equal to the inverse Fourier transform of $I_{sgl}(U,V)$.

2 Instrumentation and Theory

2.1 *Optical System to Measure PSF_{dbl}*

A photograph of the PSFAS is shown in Fig. 1, and the optical system with the alignment mechanism is shown schematically in Fig. 2. The PSFAS measurements were performed on human subjects after induction of mydriasis using atropine. An infrared superluminescent diode (SLD, 840 nm, 2-mW output, maximum quantity restricted to 20 μW incident on the eye) forms a point light source, PLS, with a 5-μm diameter. The light beam emitted by the point light source passes through a collimating lens (L1, $f=30$ mm), an artificial pupil (API), a polarized beamsplitter (PLBS), and a rotator prism (RP) before it reaches the subject's eye (SE). The light beam reflected from the subject's retina passes through the RP, the PLBS, and

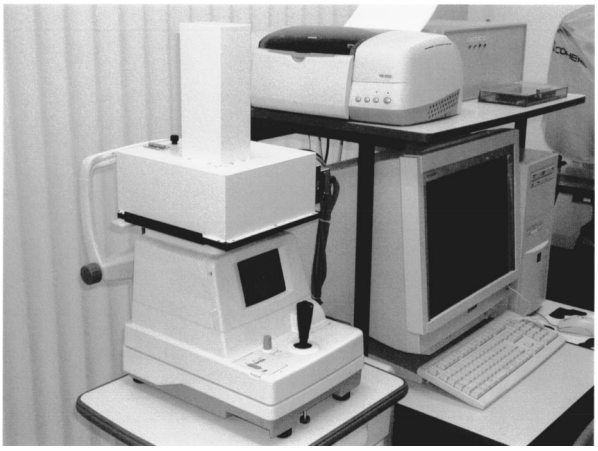

Fig. 1 External appearance of the point spread function analysis system (PSFAS).

an exit artificial pupil (APE) and is then focused with a lens (L2, $f=150$ mm) onto a CCD camera (Kodak Megaplus 1.6i). The intensity distribution of the focused spot corresponds to the PSF_{dbl}. The angular field of view on the retina was between 10 and 20 deg, with the API and the APE changing simultaneously from 3 to 6 mm.

To selectively obtain only the polarized component of the retinal reflection, a quarter-wave plate was added in front of the subject's eye to produce a beam with circular polarization. The retinal image in the creation of the model of the polarization state of the beam in each part of the optical system is shown in Fig. 3. The incident polarized beam passes through the outer limiting membrane, the photoreceptor layer, the RPE, and the choroid and reaches the sclera. The beam is partially absorbed and reflected during its path in the retina. From the studies of Williams et al.[6] we can assume that most of the energy of the beam is contained in the retinal image near the outer limiting membrane after polarized reflection by the RPE. This reflected beam maintains its polarization but

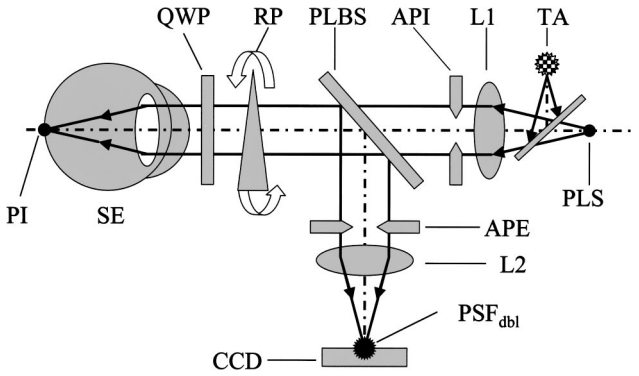

Fig. 2 Diagram of the optical system. PLS, infrared point light source; TA, auto fixation point; CCD, CCD camera; L1, collimating lens; SE, subject's eye; API, incident artificial pupil; PLBS, polarized beamsplitter; RP, rotator prism; QWP, quarter-wave plate; PI, image of point light source; APE, exit artificial pupil; L2, focusing lens; DP-PSF, double-passed PSF image. [Reprinted by permission from *Japanese Journal of Visual Science*, **21**(2), 46–53 (2002) Fig. 1. Copyright © Nihon Ganka Kiyoukai.]

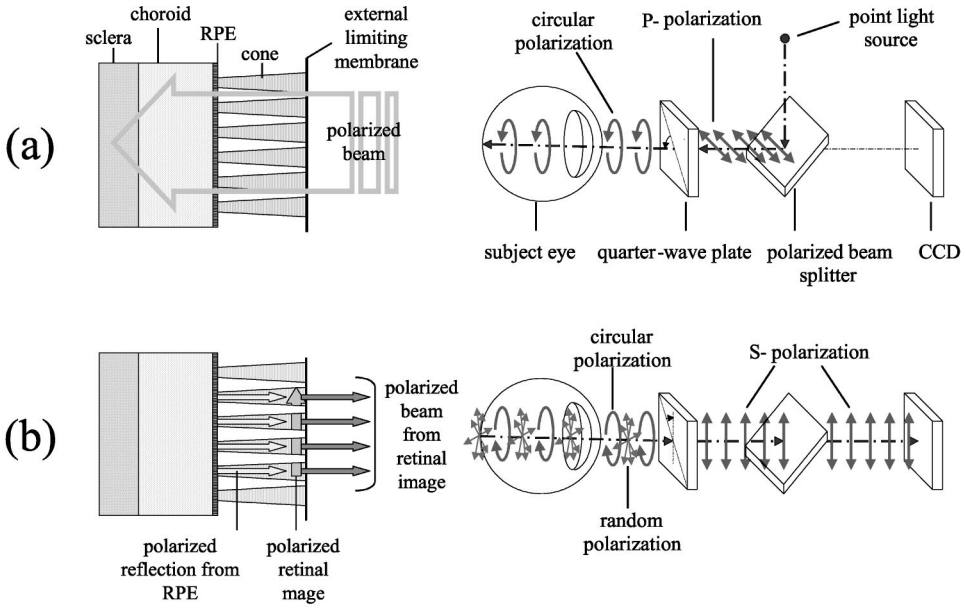

Fig. 3 Retinal image in creation of the model by the optical system for the polarized reflection component. (a) A circular polarized beam is projected to the fundus. (b) Only back-lashing circular polarized beam, which is the specular component from the fundus, can pass through the quarter-wave plate and polarized beamsplitter assembly.

loses most of its coherence when it is waveguided within the photoreceptor layer.[6] Therefore only the circularly polarized component of the retinal reflection is transmitted through the quarter-wave plate and polarizing beamsplitter. Consequently, the image recorded by the CCD camera comes only from the polarized reflection component.

Although SLDs, whose emission characteristics lie between those of laser diodes and light-emitting diodes, emit incoherent light with high directivity and high power,[17] the reflected beam from the retina preserves coherence slightly as stated previously. The PSF_{dbl} captured by the CCD camera includes a slight speckle pattern. In conventional setups, which use a coherent laser source, the laser speckle pattern is usually eliminated by averaging the recorded PSF, which requires a long exposure time. In our setup, the speckle pattern is eliminated by using the summing and averaging effect of the RP, which is a slightly tilted, plane-parallel, rotating plate with a driving frequency of approximately 5000 rpm and which places the first and second optical passes on the same path. Therefore, although the light beam passing through the RP describes small circular arcs on the subject's retinal surface at the first optical pass, the light beam passing through the RP after being reflected from the subject's retina shapes the PSF_{dbl} on the CCD camera on one fixed point during the second optical pass. As a result of this, the PSF_{dbl} captured by the CCD camera is summed and averaged, and the speckle pattern is eliminated in a short time.

2.2 *Calculation of the MTF_{sgl}*

In the PSFAS optical system, mydriasis is induced using atropine in subjects before measurements are performed. An infrared point light source then is projected onto the retina, and the PSF_{dbl} image is captured by the CCD camera. During this process, the PSF_{dbl} at each diopter is captured by L1 and L2 (Fig. 2), moving a 0.125-diopter step simultaneously. The PSF_{dbl} with the maximum Strehl ratio is then selected in the manual operation.

The MTF_{dbl} was derived by Fourier transformation of the PSF_{dbl} as follows:

$$I_{\mathrm{dbl}}(U,V) = \left| FT\{i_{\mathrm{dbl}}(x,y)\} \right|, \tag{1}$$

where FT is the Fourier transform operator.

Here we assume that the retinal image captured by the CCD camera and the point light source are mutually incoherent and that the optical system has no effect on the MTF. The SLD is a point light source (see Sec. 5). In addition, the first and the second optical paths through the retina and the optical system of the eye (Fig. 4) are identical. The RPE works as a

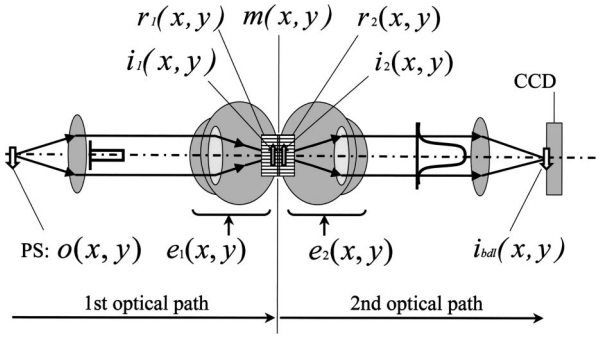

Fig. 4 Relation between the point light source $[o(x,y)]$ and the two-dimensional double-pass PSF $[PSF_{dbl}: i_{dbl}(x,y)]$ image. The beam from the point light source passes through the first optical path and then reaches the CCD camera in the second optical path after being reflected from the retina.

mirror and the photoreceptors work as a waveguide,[6] that is, the retinal reflection factor is assumed to be a complex function with unit modulus and random phase.[18]

The rationale and validity of these assumptions are addressed in Sec. 5. With these assumptions, the double-pass image captured by the CCD camera can be calculated using the following formula (Fig. 4):

$$o(x,y)\otimes e_1(x,y)\otimes r_1(x,y)\otimes m(x,y)\otimes r_2(x,y)\otimes e_2(x,y) = i_{\mathrm{dbl}}(x,y), \tag{2}$$

where $\otimes$ is the convolution, and the functions are defined as follows:
$o(x,y)$ is the spread function of the point light source
$e_1(x,y)$ is the spread function of the first optical path through the eye's optical system
$r_1(x,y)$ is the spread function of the first optical path through the retina
$m(x,y)$ is the spread function of the reflection characteristics of the retina
$r_2(x,y)$ is the spread function of the second optical path through the retina
$e_2(x,y)$ is the spread function of the second optical path through the eye's optical system.

Taking the Fourier transform of Eq. (2) yields:

$$I_{\mathrm{dbl}}(U,V)=O(U,V)\times E_1(U,V)\times R_1(U,V)\times M(U,V)\times R_2(U,V)\times E_2(U,V) \tag{3}$$

$$\{E(U,V)R(U,V)\}^2=I_{\mathrm{dbl}}(U,V). \tag{4}$$

Taking the square root of both sides of Eq. (4), we obtain:

$$E(U,V)R(U,V)=[I_{\mathrm{dbl}}(U,V)]^{1/2}. \tag{5}$$

Combining Eqs. (1) and (5), we obtain:

$$\begin{aligned} I_{\mathrm{sgl}}(U,V)&=[I_{\mathrm{dbl}}(U,V)]^{1/2}\\ &=E(U,V)R(U,V)\\ &=[|FT\{i_{\mathrm{dbl}}(x,y)\}|]^{1/2}, \end{aligned} \tag{6}$$

where $I_{\mathrm{sgl}}(U,V)$ is the single-pass MTF ($\mathrm{MTF_{sgl}}$).

Equation (6) shows that with our optical system and underlying assumptions, the $\mathrm{MTF_{sgl}}$ is equal to the square root of the Fourier transform of the $\mathrm{PSF_{dbl}}$.

2.3 *Simulation of the Optotype Image Projected onto the Neurosensory Retina*

The image of any optotype projected onto the neurosensory retina, $g(x,y)$, can be calculated as a physical representation by the following equation:

$$g(x,y)=c(x,y)\otimes i_{\mathrm{sgl}}(x,y), \tag{7}$$

where $c(x,y)$ is the spread function of the optotype, which is the image preserved in the computer memory as digital data and $i_{\mathrm{sgl}}(x,y)$ is the inverse Fourier transform of $I_{\mathrm{sgl}}(U,V)$. Using Eq. (7), the image of the arbitrary optotype can be simulated by taking the digital data of the corresponding optotype. However, this image includes some background noise that originated in the photoelectric conversion process of PSFAS and a small quantized error that is due to a discretization effect when the $\mathrm{PSF_{dbl}}$ is captured by the CCD camera and the calculating process in the computer.

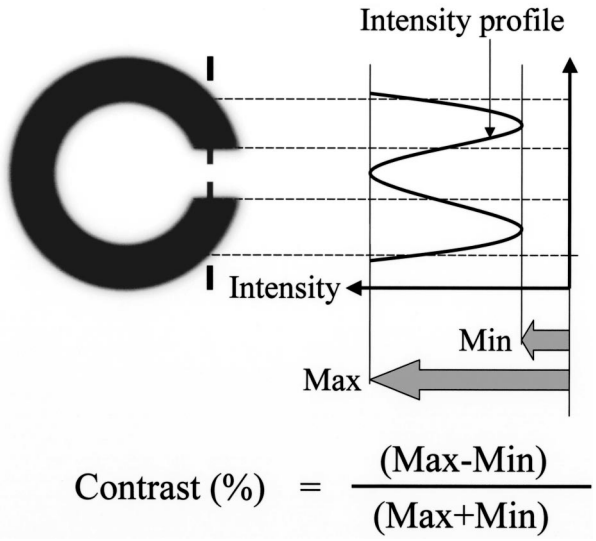

Fig. 5 The contrast intensity was determined from the intensity profiles of the gap of each simulated retinal image of the Landolt ring.

2.4 *Calculation of the Contrast Characteristics from the Simulated Optotype Image Projected onto the Neurosensory Retina*

It is not simple to understand how a subject recognizes the gap in the Landolt rings. To understand this, we must consider the contrast sensitivity function, including the transfer characteristics of the retina and brain (retina–brain system). However, only the contrast characteristics of the eye's optical system from the cornea to this side of the neurosensory retina are introduced here. To calculate the contrast characteristics, images of Landolt rings[19] of various sizes are projected onto the neurosensory retina and deduced according to Eq. (7). Then the intensity profile of each image in the gap of the Landolt rings is measured on the image preserved in the memory of the computer as digital data. The contrast (%) for each visual acuity is calculated from the maximum and minimum intensities of the intensity profile of each image (Fig. 5).

3 Validation of the $\mathrm{MTF_{sgl}}$ Measured with PSFAS

3.1 *Experimental Technique*

The $\mathrm{MTF_{sgl}}$ calculated from PSF measurements using the PSFAS was compared with the MTF calculated from a contrast sensitivity measurement using interferometry. The interferometric contrast sensitivity provides information on the entire visual system, including visual processing in the retina–brain system, whereas the $\mathrm{MTF_{sgl}}$ provided by the PSFAS includes only the optics of the eye and the retina. The MTF of the optical system of the eye and the retina ($\mathrm{MTF_E}$) is equal to the ratio of the MTF of the whole visual system ($\mathrm{MTF_A}$) divided by the MTF of the retina–brain system ($\mathrm{MTF_R}$):

$$MTF_E=MTF_A/MTF_R. \tag{8}$$

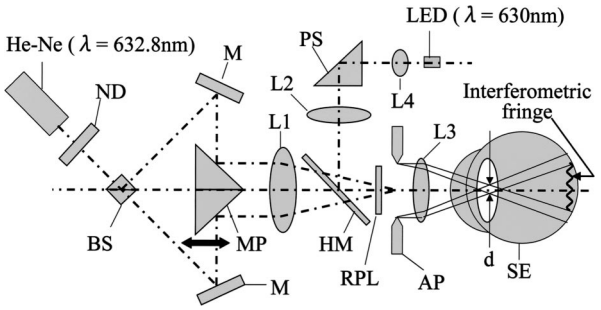

Fig. 6 Diagram of the optical system of a newly drawn interferometric contrast sensitivity system. He:Ne, helium-neon laser ($\lambda = 632.8$ nm; ND, neutral-density filter; BS, beamsplitter; MP, mirror prism; M, mirror; L1 and L3, relay lenses; HM, half mirror; RPL, rotator polarizer; AP, incident pupil; LED, light-emitting-diode ($\lambda = 630$ nm); PS, prism; L2 and L4, condenser lens; SE, subject's eye.

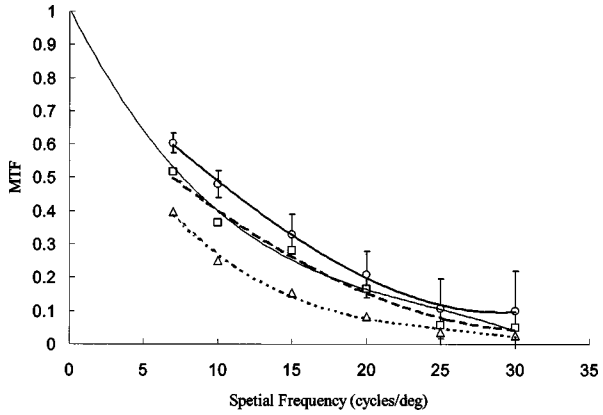

Fig. 7 Results of validation for MTF_{sgl}. Thin solid line; MTF_{sgl} in a 3-mm pupil by PSFAS. Thick solid line with open circles: MTF_E 3 mm in diameter. Thick, long-dashed line with open squares: MTF_E 4 mm in diameter. Thick, short-dashed line with open triangles: MTF_E 6 mm in diameter.

The MTF_E was calculated from the measurements of the MTF_A and the MTF_R in one 55-year-old normal human subject (T.I., emmetropic) and compared with the MTF_{sgl} provided by PSFAS. This subject was well trained for this psychophysical experiment. The artificial pupils (APE and API in Fig. 2 of the PSFAS) at 3, 4, and 6 mm were put in place when the MTF_{sgl} was measured.

The MTF_A was measured subjectively with a system developed by Kawahara[20] and Kawahara and Owasasa[21] (Takagi MT390). Sinusoidal gratings of the various spatial frequencies with modulation amplitudes that vary logarithmically in the vertical direction were used as test patterns. These patterns are transmitted illuminated by a white light source. During the test, the subject was asked to indicate the boundary of the grating, which corresponds to the position where the patient can barely detect the grating modulation. The value of the modulation at this boundary corresponds to the modulation threshold of the subject at the corresponding spatial frequency. The MTF curve was obtained using seven test plates with different spatial frequencies. The maximum frequency was 43.6 cycles/deg at a viewing distance of 2 m. The artificial pupils at 3, 4, and 6 mm were placed in front of the subject's eye when this MTF_A was measured.

On the other hand, the MTF_R was measured with a custom-made interferometric contrast sensitivity method that we constructed based on the original design and validation by Campbell and Green in 1965.[22] This system allows forced-choice contrast sensitivity measurements without blurring by the optics of the eye.[6] The optical arrangement of the system is shown schematically in Fig. 6. The light beam from the He:Ne laser ($\lambda = 632.8$ nm), which is divided by a beamsplitter (BS), forms two secondary point light sources in the pupil of the subject's eye (SE). Interferometric fringes are formed on the retina by interfering with each secondary point light source the frequency unit of the interferometric fringe on the retina is indicated by distance d, which is changed by moving the mirror prism (MP). The contrast of the interferometric fringe is indicated by the intensity ratio to background illuminance by the light-emitting diode (LED) ($\lambda = 630$ nm).

Young's interferometric fringes were formed on the retina in Maxwellian view using visible light. To measure the MTF_R using this system, the illumination intensity on the retina was kept constant and the frequency of the interferometric fringes was varied. Frequency unit f of the interferometric fringe on the retina is given by the fundamental relationship:

$$f = d\pi/180\lambda\,(\text{cycles/deg}), \tag{9}$$

where d is the distance between two secondary point light sources, which is varied by moving the mirror prism (MP) horizontally. Technical issues involved in this method are described in the literature.[6] In addition, MTF_A and MTF_R were measured with the retinal illuminance maintained at the same level.

3.2 *Results*

The MTF_{sgl} measured in a 3-mm pupil and the MTF_E in a 3-mm pupil are shown in Fig. 7. The experimental result of the MTF_E shown was the average of five measurements. To clarify the reproducibility of the measurements, the standard deviation of multiple measures in a 3-mm pupil is shown. The standard deviation increases as the frequency increases, because it is more difficult for a subject to recognize the high-frequency interferometric fringe formed on the retina than the low-frequency interferometric fringe. The MTF_E in a 3-mm pupil calculated from Eq. (8) is almost equal to the MTF_{sgl} in a 3-mm pupil measured and calculated using the PSFAS in the frequency range from 8 to 30 cycles/deg. The MTF_E in the 4-mm and the 6-mm pupils was slightly lower than that of the 3-mm pupil. It is conceivable that this phenomenon is the result of the spherical aberration that increases gradually with increased pupil diameter. In addition, there is still a slight gap between the MTF_{sgl} and MTF_E in a 3-mm pupil that could be due to the different wavelengths of the MTF_{sgl} at 840 nm and the MTF_E at 632.8 nm. Considering these conditions, the results imply that the MTF_{sgl} provided by the PSFAS represents the optical characteristic of the entire optical system from the cornea to the entrance of the neurosensory retina.

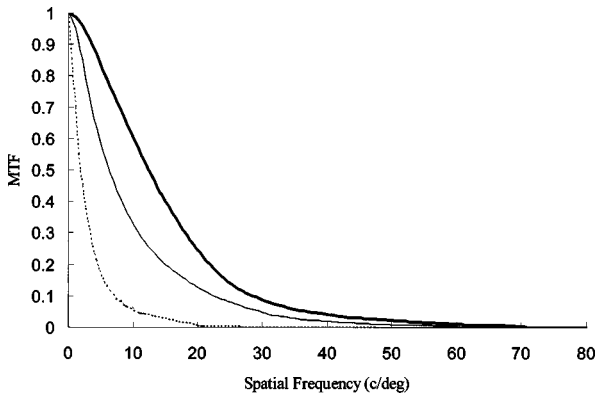

Fig. 8 MTF_{sgl} in several subjects with a 4-mm pupil. Thick solid line: subject Y.T., 23-year-old emmetrope. Thin solid line: subject S.N., 60-year-old. Dashed line: subject Y.M., 84-year-old with an age-related cataract.

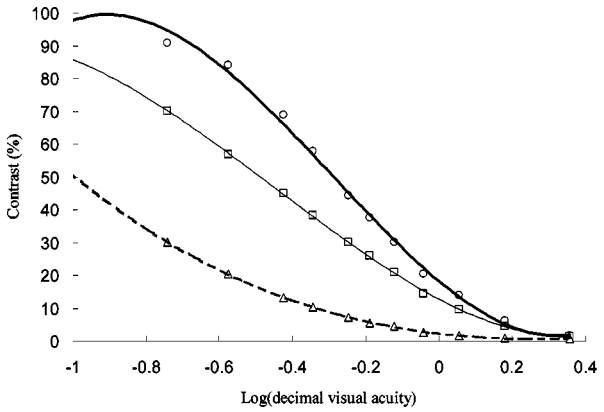

Fig. 10 Contrast characteristics in several subjects with a 4-mm pupil. Thick solid line with open circles: subject Y.T., 23-year-old emmetrope. Thin solid line with open squares: subject S.N., 60-year-old. Dashed line with open triangles: subject Y.M., 84-year-old with an age-related cataract.

4 Clinical Application Examples: Normal and Cataractous Eyes

The PSFAS was used to measure the MTF_{sgl},[11] simulated retinal images, and contrast characteristics of three subjects (Y.T., age 23, emmetropic; A.Y., age 60, fully corrected myopic astigmatism; and Y.M., age 84, age-related cataract). The cylindrical refractive error of patient A.Y. was corrected using trial lenses and the spherical refractive error was corrected by adjusting the position of lens L1 and lens L2 (Fig. 2) to maximize the Strehl ratio at the PSF_{dbl} captured by the CCD camera. The artificial pupils (APE and API) of the PSFAS were fixed at 4 mm during all measurements. Figure 8 shows the MTF_{sgl} of each subject and demonstrates the tendency for degradation with aging and rapidly decreasing optical performance. This feature is seen clearly in the simulated retinal images (Fig. 9) and in the contrast characteristics (see Sec. 2.4) (Fig. 10), which are concave in the subject with cataract and convex in the younger and 60-year-old subject in the midfrequency range. These results imply that even though all three subjects can see the gaps in the same Landolt rings, the quality of vision of the subject with a cataract is reduced because the image contrast is reduced. These results were ob-

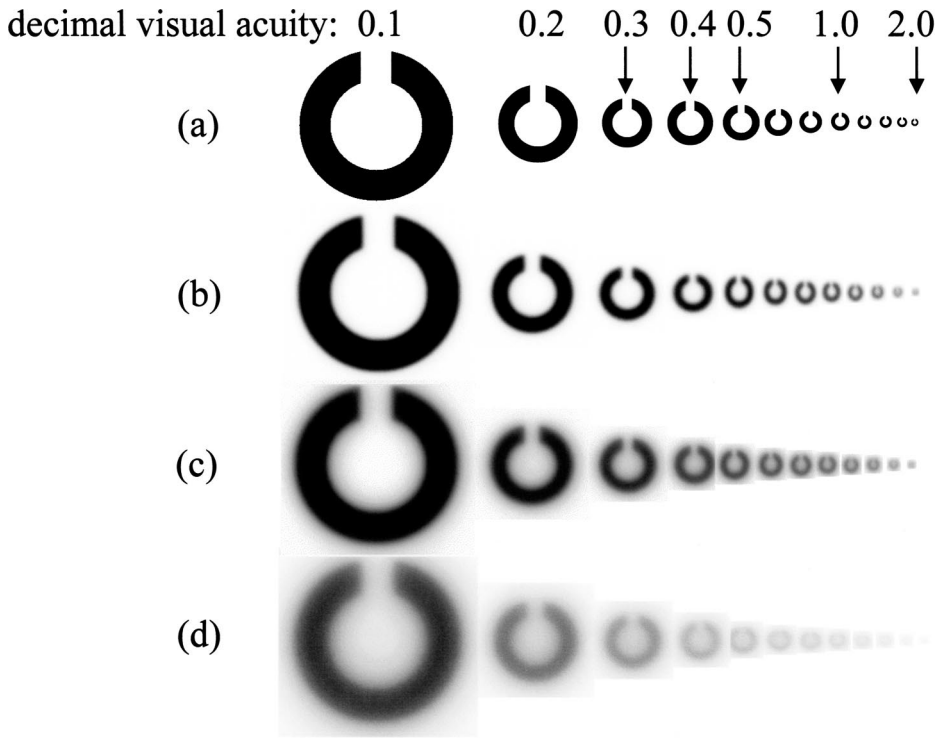

Fig. 9 The simulated retinal images in several subjects with a 4-mm pupil. (a) Original optotypes. (b) Subject Y.T., 23-year-old emmetrope. (c) Subject S.N., 60-year-old. (d) Subject Y.M., 84-year-old with an age-related cataract.

tained by gaining a true knowledge of the features of degradation of the eye's optical performance by haze and scattering in the ocular media originating with cataract.

5 Discussion

We developed a system that measures the ocular PSF_{dbl} and calculates the corresponding MTF_{sgl} and simulated retinal images. This system was helpful in quantifying factors, such as lower contrast, that affect visual quality but cannot be detected solely by measurements of resolution limits. Practically, although several investigators have reported the relation between scatter or haze and retinal image degradation in cataract,[23,24] the PSFAS system can predict the retinal image quality more clearly by synthesizing optotype images, which includes the effect of haze and scattering in an eye with cataract. In the calculation of the MTF_{sgl}, we assumed that the effect of the PSFAS optical system is small enough to be ignored. Indeed, owing to the finite size of the photoreceptors, the spatial sampling rate at the retina of the subject's eye is 120 cycles/deg. On the other hand, the magnification of the optical system that projects the retinal image onto the CCD camera is $\times 8.5$ and the CCD pixel size is 9 μm. With these values, the finite size of the point light source does not contribute to the MTF_{dbl}. Simulation using ray-tracing software during the lens design stage confirmed that the combined MTF of the PSFAS optical system together with an aberration-free model eye was, for all practical purposes, equal to the MTF of the aberration-free model eye.

The other underlying assumption in the calculation of the MTF_{sgl} is that the relations between the point light source, the image on the retina, and that on the CCD camera image are mutually incoherent. The retinal image and the PSF_{dbl} captured by the CCD camera in Fig. 2 can be assumed to be mutually incoherent because the PSF_{dbl} is captured through a high-speed rotating prism that produces an incoherent average and greatly reduces the coherence of the PSF_{dbl}. This image is waveguided within the photoreceptors, which act as waveguides that preserve polarization but do not preserve the phase information between the neighboring photoreceptors.[25] Accordingly, the polarized retinal image and the point light source[26] are also mutually incoherent.

One of the potential limitations of the PSFAS is that the simulated retinal images might not correspond exactly to the real retinal images because the MTF_{sgl} that was derived by the double-pass method does not preserve the phase transfer function. In other words, the contributions of odd aberrations to the phase term of the optical transfer function in the first and second optical paths are equal but opposite to each other and thus cancel each other out.[27,28]

Nevertheless, using the PSFAS, the simulated retinal images and the contrast characteristics calculated from the simulated retinal images almost agree with the real ones in subjects who were not greatly affected by odd aberrations such as keratoconus. In addition, the single-pass MTF provided by the PSFAS was also found to agree well with the MTF of the eye's optical system derived from alternative measurement techniques. These findings indicate that the MTF_{sgl} provided by the PSFAS is a reliable estimate of the optical response of the eye from the cornea to the entrance of the neural visual system.

The difference in wavelength between the near-infrared light source that is used in PSFAS for obtaining the MTF_{sgl} and the visible light source that was used for measuring MTF_A and MTF_R may have contributed in part to the slight differences that were observed in the MTF_E provided by both techniques.

6 Conclusions

We present an optical system, a PSFAS, that calculates the ocular MTF from measurements of the double-pass PSF, using polarized light to select the polarized component of retinal reflection and a high-speed rotating prism to reduce the coherence of the PSF. Our experiments demonstrate that the MTF_{sgl}-simulated retinal image and contrast characteristics provided by the PSFAS are reliable estimates of the performance of the eye's optical system from the cornea to the entrance of the neural visual system. Our preliminary clinical results indicate that it is necessary to consider the contrast sensitivity function when investigating visual performance.

Acknowledgments

We are grateful to Jean-Marie Parel and Fabrice Manns from the University of Miami for their help in preparing the manuscript. I also thank the reviewers for valuable and very instructive advice.

References

1. J. Santamaria, P. Artal, and J. Bescos, ''Determination of the point-spread function of human eyes using a hybrid optical-digital method,'' *J. Opt. Soc. Am. A* **4**(6), 1109–1114 (1987).
2. P. Artal, M. Ferro, I. Miranda, and R. Navarro, ''Effects of aging on retinal image quality,'' *J. Opt. Soc. Am. A* **10**(7), 1656–1662 (1993).
3. R. Navarro and M. Ferro, ''Modulation transfer functions of eyes implanted with intraocular lenses,'' *Appl. Opt.* **32**(31), 6359–6367 (1993).
4. P. Artal and R. Navarro, ''Monochromatic modulation transfer function of the human eye for different pupil diameters: an analytical expression,'' *J. Opt. Soc. Am. A* **11**(1), 246–249 (1994).
5. P. Artal, I. Iglesias, N. Lopez-Gil, and D. G. Green, ''Double-pass measurements of the retinal-image quality with unequal entrance and exit pupil sizes and the reversibility of the eye's optical system,'' *J. Opt. Soc. Am. A* **12**(10), 2358–2366 (1995).
6. D. R. Williams, D. H. Brainard, M. J. McMahom, and R. Navarro, ''Double-pass and interferometric measures of the optical quality of the eye,'' *J. Opt. Soc. Am. A* **11**(12), 3123–3135 (1994).
7. D. R. Williams, G. Y. Yoon, J. Porter, A. Guirao, H. Hofer, and I. Cox, ''Visual benefit of correcting higher order aberration of the eye,'' *J. Refract. Surg.* **16**, S554–S559 (2000).
8. W. N. Charman, ''Reflection of plane-polarized light by the retina,'' *Br. J. Physiol. Opt.* **34**, 34–49 (1980).
9. G. J. Blokland and D. Norren, ''Intensity and polarization of light scattered at small angles from the human fovea,'' *Vision Res.* **26**, 485–494 (1986).
10. W. N. Charman, ''Some sources of discrepancy between static retinoscopy and subjective refraction,'' *Br. J. Physiol. Opt.* **30**, 108–118 (1975).
11. W. N. Charman and J. A. M. Jennings, ''Objective measurements of the longitudinal chromatic aberration of the human eye,'' *Vision Res.* **16**, 999–1005 (1976).
12. D. O'Leary and M. Millodot, ''The discrepancy between retinoscopic and subjective refraction: effect of light polarization,'' *Am. J. Optom. Physiol. Opt.* **55**, 553–556 (1978).
13. K. Kobayashi, M. Shibutani, G. Takeuchi, K. Ohnuma, and Y. Miyake, ''Measurement of the single-pass modulation transfer function of the human eye by specular reflection point spread function,'' *Jpn. J. Vis. Sci.* **21**(2), 46–53 (2001).
14. K. Kobayashi, M. Shibutani, G. Takeuchi, K. Ohnuma, Y. Miyake, K. Negishi, K. Ohno, and T. Noda, ''Simulation of the retinal image of

the human eye and prediction of the visual acuity using point spread function,'' *Jpn. J. Vis. Sci.* **21**(3), 85–92 (2001).
15. K. Kobayashi, M. Shibutani, G. Takeuchi, K. Ohnuma, Y. Miyake, K. Negishi, K. Ohno, and T. Noda, ''A comparison of scattering reflection and specular reflection for double-pass MTF of the human eye,'' *Invest. Ophthalmol. Visual Sci.* **42**(4), S161 (2001).
16. K. Kobayashi, M. Shibutani, G. Takeuchi, K. Ohnuma, Y. Miyake, K. Negishi, K. Ohno, and T. Noda, ''Prediction of defocusing visual acuity using square-wave MTF in human eyes,'' Abstract 2009, The Association for Research in Vision and Ophthalmology Annual Meeting (2002).
17. O. Mikami, ''Optical characteristics and applications of super luminescent diode,'' *J. Opt. Jpn.* **3**, 143–149 (1990).
18. P. Artal, S. Marcos, R. Navarro, and D. R. Williams, ''Odd aberration and double-pass measurements of retinal image quality,'' *J. Opt. Soc. Am. A* **12**(2), 195–201 (1995).
19. R. B. Rabbetts, *Clinical Visual Optics*, 3rd ed., pp. 19–61, Butterworth-Heinemann, Oxford (1998).
20. T. Kawahara, ''Modulation transfer function and visual function,'' *Ganka* **23**, 1043–1054 (1981).
21. T. Kawahara and D. Owasasa, ''A simple method for the modulation transfer function of the human visual system,'' *Rinsho Ganka* **33**(12), 1505–1509 (1979).
22. F. W. Campbell and D. G. Green, ''Optical and retinal factors affecting visual resolution,'' *J. Physiol. (London)* **181**, 576–593 (1965).
23. L. T. Chylack, J. K. Wolfe, and D. M. Singer, ''The lens opacities classification system III,'' *Arch. Ophthalmol. (Chicago)* **111**, 831–836 (1993).
24. H. Karbassi, P. C. Magnante, J. K. Wolfe, and L. T. Chylack, ''Objective line spread measurement, Snellen acuity, and LOCS II classification in patients with cataract,'' *Optom. Vision Sci.* **70**, 986–962 (1993).
25. G. J. Blokland, ''Ellipsometry of the human retina in vivo: preservation of polarization,'' *J. Opt. Soc. Am. A* **2**, 72–75 (1985).
26. G. J. Blokland and D. Norren, ''Intensity and polarization of light scattered at small angles from the human fovea,'' *Vision Res.* **26**, 485–494 (1986).
27. H. C. Howland and B. Howland, ''A subjective method for the measurement of monochromatic aberrations of the eye,'' *J. Opt. Soc. Am.* **67**, 1508–1518 (1977).
28. C. W. Campbell and E. M. Harrison, ''Psychophysical measurements of the blur on the retina due to the optical aberrations of the eye,'' *Vision Res.* **30**, 1587–1602 (1990).